www.rericjournal.ait.ac.th

Optimization Design Procedure of a Radial Impulse Turbine in OWC System

Khalid Elatife*,[1] and Abdellatif El Marjani*

Abstract – *Wave energy exploitation is of great interests nowadays due to its sustainability, reliability and large potential. This paper aims to firstly represent the turbine designs used in oscillating water column (OWC) system for wave energy conversion, and secondly to improve the rotor blade performances of a bidirectional radial impulse turbine which is in use in this system. Symmetrical blade profile based on use of circular arcs and straight lines has been adopted. A new procedure for optimizing the geometrical blade parameters has been introduced in this work. The design of experiments (DOE) method has been adopted with four blade geometrical parameters and two levels for reducing the number of numerical tests to determine the optimal profile in order to maximize and equilibrate the efficiency between exhalation and inhalation modes. Numerical tests in the whole turbine geometry have been carried out with ANSYS FLUENT 15.0. Significant differences have been noticed by varying the rotor blade profile. A flow analysis for the duct and the turbine elements; IGV, rotor and OGV has been performed. Performances of the turbine equipped with rotor designed with circular profiles in the present study have been compared to those of a previous design based on use of elliptical profiles. An increase of about 18% in terms of the peak efficiency in the inhalation mode has been noted for the improved design, and the performances have been equilibrated in both mode; inhalation and exhalation.*

Keywords – design of experiments method, impulse radial turbine, OWC device, rotor blade profile optimization, wave energy.

1. INTRODUCTION

Wave energy is considered as the most potential renewable and sustainable energy resources in the world. The total theoretical wave energy potential is estimated to be 29,500 TWh/yr in the world [1], and for about 700 to 900 TWh/y in the Moroccan coastlines [2]. For that, great research and development efforts has been made during the last decades in order to extract this huge energy potential for covering the continuous growing of the human energy needs.

Several energy system converters was introduced for extracting this energy, especially the oscillating water column (OWC) which is the most used system due to its low cost of installation and the simplicity of its maintenance.

An OWC device (Figure 1) is composed mainly of three elements: air chamber, air turbine and electrical generator. The first component is used to convert wave energy to pneumatic one; the second is used to convert this pneumatic energy to mechanical energy which is finally converted to electrical energy in the generator. Since 1990, Several OWC devices are construct and are still operating, such as the Picot plant in Azores, Portugal and the LIMPET plant in Islay, Scotland and other plants [3].

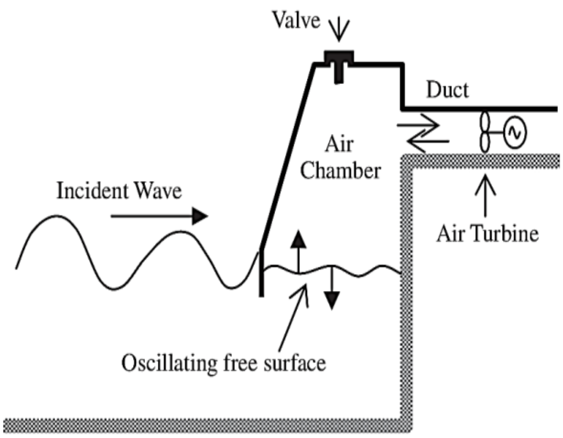

Fig. 1. The oscillating water column system (OWC).

The turbine element, that equips the OWC system, should rotate in one direction despite of the air direction changes due to the water oscillating inside the air chamber. The first turbines used in the OWC prototypes are the Wells type turbines [4]. However, through exploitation of this turbine, some drawbacks have been confronted [5], such as: poor starting characteristics, high speed operation, high efficiency in a narrow range of flow rates, high periodical axial thrust, high noise level, and finally the crucial problem of stall. In order to overcome these disadvantages, an alternative type turbine was introduced by Babinstev [6], which is an impulse type turbine.

Two alternative types of impulse turbine have been introduced, the axial and the radial one [7]-[8]. According to research investigations, it has been found that the radial impulse turbine has some advantages compared to the axial one in terms of low manufacturing cost, absence of the oscillating axial

*Turbomachinery Laboratory, EMISys Research Team, Engineering 3S Research Center, Mohammadia School of Engineers, University Mohammed V, Rabat, Morocco.

[1]Corresponding author;
Tel: + 212 613114720
E-mail: khalid.elatife@gmail.com.

thrust and high torque due to the radial configuration design [9].

According to investigation results of reference [10], improved performances can be obtained in both operating modes (inhalation and exhalation) by modifying the aerodynamic design of the inner guide vanes in the radial impulse turbine. A model of this improved turbine has been manufactured and installed at the EMI' Turbomachinery Laboratory for experimental tests. An alternative design of the axial impulse turbine have been introduced [11] in which the solution consists of coupling two turbines working in a twin configuration for optimizing the efficiency in both operating modes; inhalation and in exhalation. Significant improvements in the efficiency have revealed from the experimental tests. Other design corresponding to a varying radius model of the axial impulse turbine has been also introduced in order to reduce the energetic losses and consequently increase the efficiency [12]. A bi-radial turbine has been introduced for which a notable increasing in efficiency (close to 80 %) has been reached [13]-[14]. Recently, a novel turbine with twin-rotor has been designed in [15] and a peak efficiency of about 85% has been obtained. Some recent optimization studies have been performed to improve the impulse turbine performances, as presented in the review [16].

The objective of this paper is to implement the design of experiments (DOE) method [17] for optimizing the rotor blade geometry of a radial impulse turbine. The stator parameters are fixed and based on the values of [18].The flow in modified geometries has been simulated by using ANSYS FLUENT 15.0 for efficiency computation. In the present work, a new rotor blade design with circular profiles is adopted. This blade profile consists of using a symmetrical profile with two circular arcs and two straight lines at the leading and trailing edges. The profile optimization design is based on drawing up the DOE method on the basis of four parameters as depicted in Figure 3: the radius of the suction side, the chord, and the inter-centres distance of the two circular arcs and the geometrical angle in the leading and trailing edges of the blade rotor. In this work, an optimized rotor blade design that maximizes and equilibrates the turbine efficiency on inhalation and exhalation (both) modes will be presented. A flow analysis in the different turbine elements has been conducted for losses understanding. A performance comparison between the turbines designed with circular profiles and elliptical profiles [10] for the rotor element has been also performed. An increase of about 18 % for the average efficiency has been reached for the optimized radial impulse turbine with a circular profile. A peak efficiency of 68.5% in inhalation mode has been reached.

2. ROTOR BLADE OPTIMIZATION OF A RADIAL IMPULSE TURBINE

The turbine is composed of a rotating part, the rotor, and a fixed part, the stator, as depicted in Figure 2. Since the turbine turns in one direction despite the air flow the bidirectional, it is equipped with a single rotor of symmetrical blades, one row of inner guide vanes (IGV) and one row of outer guide vanes (OGV).

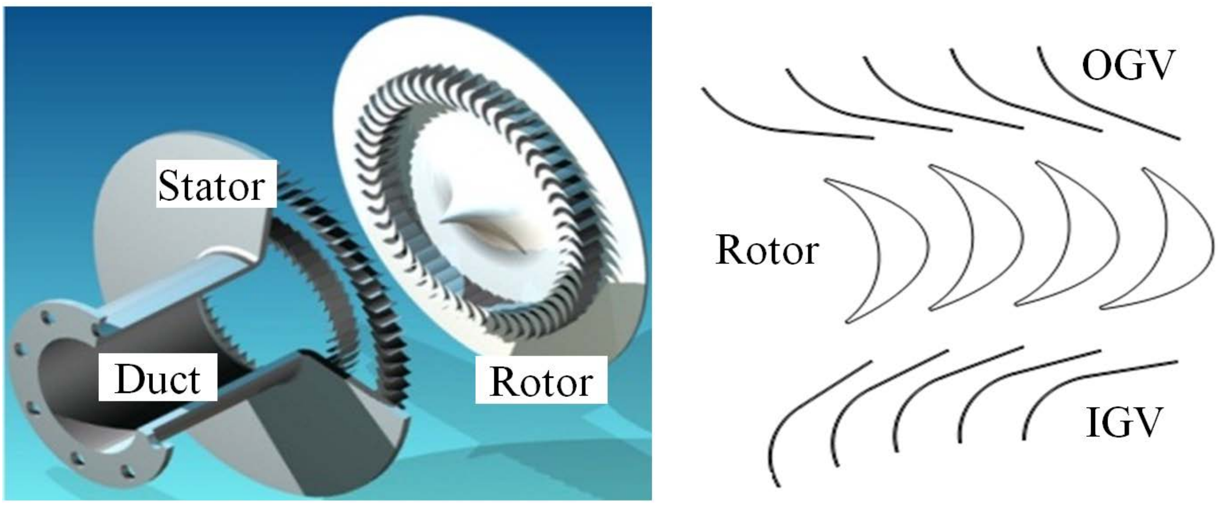

Fig. 2. Rotor and stator of radial impulse turbine [10]-[19].

The global efficiency of the OWC device depends on the efficiency at each phase of its energy conversion chain. For high OWC performances, great attention should be paid in the design of the turbine [19].

Setogushi *et al.* [14] has introduced and experimented a rotor blade geometry of the impulse radial turbine, composed of a circular form in the pressure side and an elliptic in the suction side [18]. Results revealed important influences of geometrical parameters such as the setting angle and others on the turbine performances. A maximal efficiency less than 30 % has been reported. A brief comparison between two rotor blade designs has been done in [20], one with elliptic shape and the other with circular arcs and four straight lines. From experimental tests, the first design has been found more efficient. However, blade profile based on circular forms can also be efficient in terms of pressure loss minimization as discussed in [21] and presents advantages in relation with the simplicity of its designing and manufacturing.

2.1 Rotor Blade Profile Description

In the present work, a symmetrical rotor blade profile with circular arcs and two straight lines has been adopted. The design parameters l_r , d_c , β^*, R_p^r and R_s^r are the chord length, the inter-distance between the circular arc centres of the pressure side O_p and the suction side O_s, the geometrical angle for two sides of the rotor blade, the radius of the pressure side arc and the radius of the suction side arc, respectively (Figure 3). In order to keep a constant passage width between consecutive rotor blades w_r, the radii R_p^r and R_s^r has been joined by the following relationships:

$$R_s^r = {}^3/_2\, w_r \text{ and } R_p^r = {}^5/_2\, w_r \tag{1}$$

Or in other form: $R_s^r = {}^3/_5\, R_p^r$

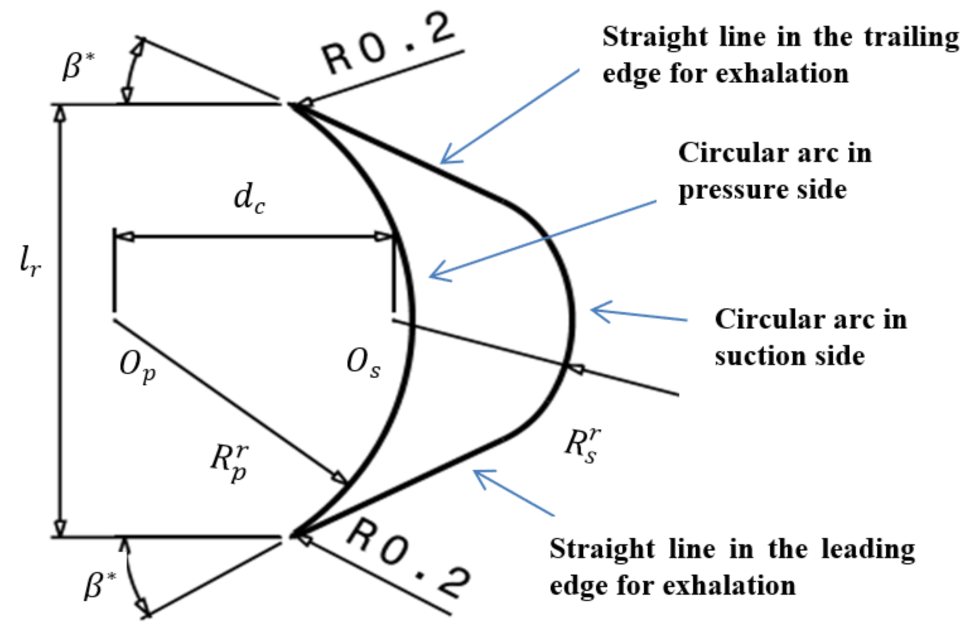

Fig. 3. A schematic of rotor blade design.

Numerical simulations will be performed for optimizing this rotor blade profile in terms of efficiency improvements. The optimization procedure is based on the use of the DOE method in order to maximise the global efficiency of the turbine as it will be detailed in the next section.

2.2 Experimental Design Method

2.2.1 Numerical flow simulation

Since the objective is to determine the rotor geometry with optimal efficiency, the viscous flow characteristics in the whole turbine geometry should be determined. In order to validate the effectiveness of this approach and reducing the computation efforts, we have considered performing analyses on 2D turbine geometry (Figure 4). For the following turbine performance evaluation section, the 3D simulations are used to perform a complete flow analysis. In the present work, the required 2D simulations tests used in the optimization process have been performed with ANSYS FLUENT as a numerical tool. Flow is considered incompressible, viscous, 2D and steady. Since the turbine is composed of rotating and fixed components (Figure 2), the sliding mesh technique has been used to manage the relative movement between the fixing and the moving part of the turbine. An unstructured triangular mesh of about 50 000 cells is used in the flow domain (Figure 4). The flow model solves the incompressible conservation equations by using a segregated solver. The flow turbulence is modelled by the standard k-ε model. The coupled conservation equations of mass, momentum and energy are solved using a segregated solver. The SIMPLEC algorithm is adopted to perform the pressure-velocity coupling.

The performance of the studied impulse turbine under steady conditions is evaluated by the following parameters:

Flow coefficient,

$$\varphi = V_r/U_r \tag{2}$$

Input coefficient,

$$C_A = \frac{2\Delta P}{\rho(V_r^2 + U_r^2)} \tag{3}$$

Torque coefficient,

$$C_T = \frac{2T}{\rho(V_r^2 + U_r^2)A_r R_r} \tag{4}$$

Efficiency,

$$\eta = (T\omega)/\Delta PQ = C_T/(C_A\, \varphi) \tag{5}$$

Where $V_r = Q/A_r$, U_r, ΔP, φ, T, A_r, R_r, ω and Q refers respectively to mean radial velocity at R_r, blade circumferential velocity at R_r, total pressure drop, air density, turbine torque, turbine flow passage area, mean radius of the rotor, rotational speed and volume flow rate. For the present study, the numerical tests serve to determine the shaft power for different flow coefficients in the two modes; exhalation and inhalation.

The adopted boundary conditions correspond in exhalation mode for different flow coefficients to a uniform mass flow rate at the inlet (the mass flow rates 0.19 kg/s, 0.38, 0.57, 0.76 and 0.96 correspond respectively to the flow coefficients 0.5, 1, 1.5, 2 and 2.5) and a uniform static pressure (0 bar) at the outlet. The rotational velocity of the rotor is fixed to ω=234 rpm. The shear condition of non-slip is adopted for all the stationary walls. For ensuring the static pressure field compatibility in the pressure outlet boundary condition, the radial equilibrium pressure distribution has been adopted. The condition of non-slip is adopted for all the walls.

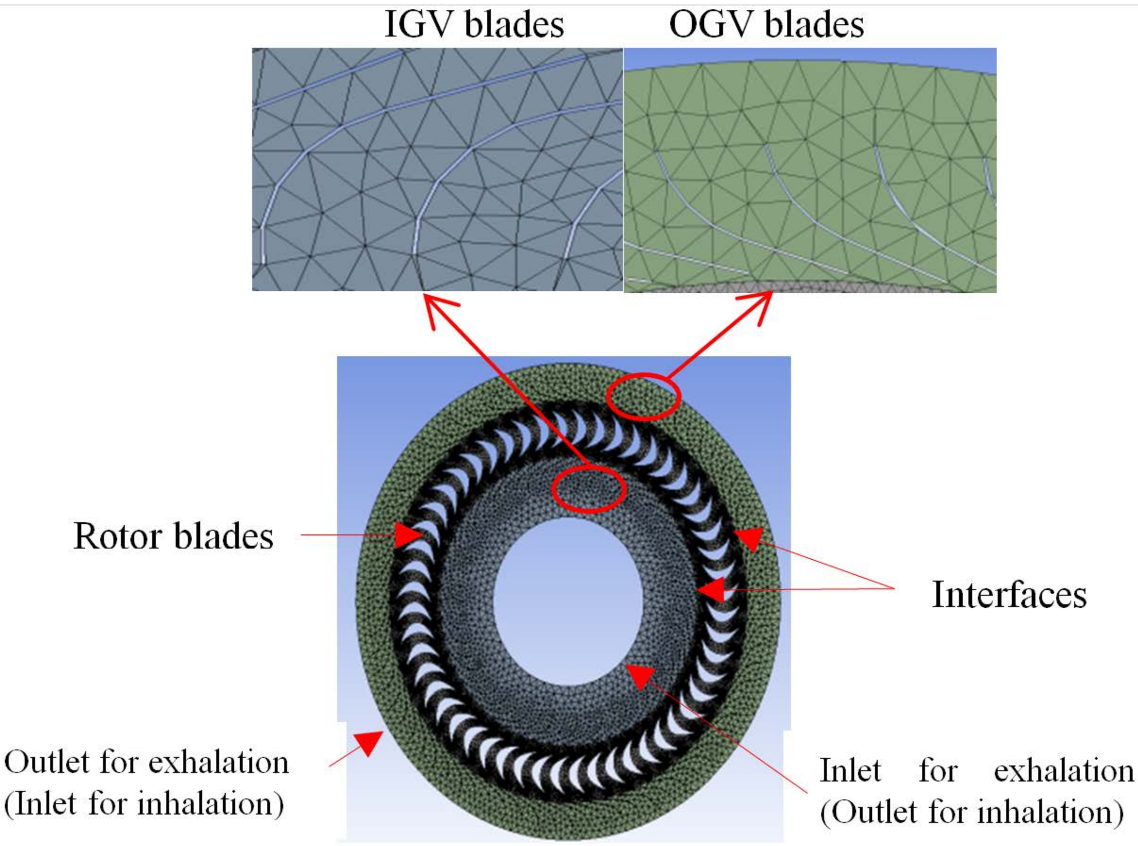

Fig. 4. 2D flow domain.

2.2.2 DOE method

The DOE method is considered for optimization of this new rotor blade design. In a first step, the DOE optimization procedure has been applied only to the rotor blade. The others blades for example the inner and the outer fixed guide vanes are kept unchanged [14]. The rotor blade analyses are based on the variation of the four input design parameters: l_r , d_c , β^*, R_p^r (see Figure 3).

For the present study, the output parameter of DOE tests is the turbine efficiency for different flow coefficients in the two modes; exhalation and inhalation.

2.2.3 The mathematical model

The mathematical model for efficiency dependency on the chosen geometrical parameters is as following:

$$\eta = a_1 + a_2 R_p^r + a_3 l_r + a_4 \beta^* + a_5 d_c \qquad (6)$$

In which: a_i, i=1…5 are variable effects to be determined for each design in both modes of turbine operation (Exhalation and Inhalation). Equation 6 will be used for the optimized geometrical parameters.

2.2.4 Initial blade rotor geometry design

For implementing the DOE method, two levels has been adopted in the present work for each geometrical parameter in order to minimize the number of simulation tests and to detect the sensitivity of each parameter on the turbine efficiency. The lower and the higher level are indexed respectively by (-1) and (1). For carrying out the first experimental design, initial rotor geometry has to be determined with fixing the number of levels of each parameter and their values. These level values has been fixed and non-dimensionalised according to [18] and to general drawings rules for turbomachinery blades. Results are shown in Table 1.

Table 1. Parameter level values for the initial DOE (dimensionless values).

Level	R_p^r	l_r	β^*	d_c
-1	0.436	0.818	25°	0.545
1	0.545	1	35°	0.6

Table 2. HADAMARD matrix for four parameters and two levels.

N°	R_p^r	l_r	β^*	d_c
Test 1	1	1	1	-1
Test 2	-1	1	1	1
Test 3	-1	-1	1	1
Test 4	1	-1	-1	1
Test 5	-1	1	-1	-1
Test 6	1	-1	1	-1
Test 7	1	1	-1	1
Test 8	-1	-1	-1	-1

Table 3. Turbine efficiency (%) for the eight tests with the initial DOE.

	Tests:	1	2	3	4	5	6	7	8
	Efficiencies:	η_1	η_2	η_3	η_4	η_5	η_6	η_7	η_8
inhalation	Flow rate: φ -0.5	46	52.8	49	54	59	46	52.8	54
	-1	50	52.7	50	54.3	58	51.6	54.3	56
	-1.5	50	52.3	49	51.4	54,9	50	55	52
	-2	49	51.1	48	50	52	49	50	51
	-2.5	48	50	47	48	50	47	49	49
Exhalation	0.5	57.6	58	61	46	49	55.8	58	59.5
	1	63	55.2	62	47	51	61	59.8	60.3
	1.5	60	54	60	48	51	58.5	57	58.8
	2	55	52,5	58	46	49	55	55,9	57
	2.5	51	51.2	56	46	48	53.4	53.9	55.4

Table 4. Coefficients a_i, i=1,…,5 for the initial DOE.

	φ	a_1	a_2	a_3	a_4	a_5
inhalation	-0.5	52	-2.3	2.74	-0.9	0.29
	-1	56	-2.8	2.14	-0.5	0.34
	-1.5	55	-1.5	1.61	0.11	1.49
	-2	52	-1.8	0.96	0.91	1.31
	-2.5	50	-1.6	0.74	0.69	1.19
Exhalation	0.5	54	-1.2	-0.1	3.09	0.72
	1	58	-0.9	0.82	3.05	0.72
	1.5	56	-0.7	0.73	2.71	0.89
	2	54	-0.8	0.52	2.52	0.72
	2.5	53	-0.7	0.26	2.24	0.74

With two (2) levels and four (4) parameters, 24 (16) tests should be carried out for a complete analysis. However, with the use of the DOE method, instead of using an exhaustive experimental design which needs large number of experiments, it is possible to perform an optimized experimental design [17] that needs lesser tests, by a formulation based on the matrix of Hadamard [22] that needs just 8 tests for this case. The elements of this matrix are presented in the Table 2.

Since 8 tests should be carried out, a matrix system is used for a compact formulation as following:

$$[\eta] = [H][A] \quad (7)$$

With: $[\eta]^t = [\eta_1, \dots, \eta_8]$ is the turbine efficiency vector of the tests; $[A]^t = [a_1, \dots, a_5]$ is the coefficient vector to determine; $[H]$ is the 8x5 Hadamard matrix in which the first column is set to unity. For each test, values of the efficiency are determined with the flow simulation in the considered geometry; the corresponding coefficients a_i can be determined by inverting simply the algebraic system (7).

2.2.5 Results of initial geometry

The efficiency results of the eight tests obtained from the numerical simulations in both turbine operation modes; inhalation and exhalation are presented in Table 3. In the all tests, the rotor rotational speed ω is of 234 rpm.

From (7), the coefficients a_i , i=1,…,5 are calculated and presented in Table 5 for the two modes.

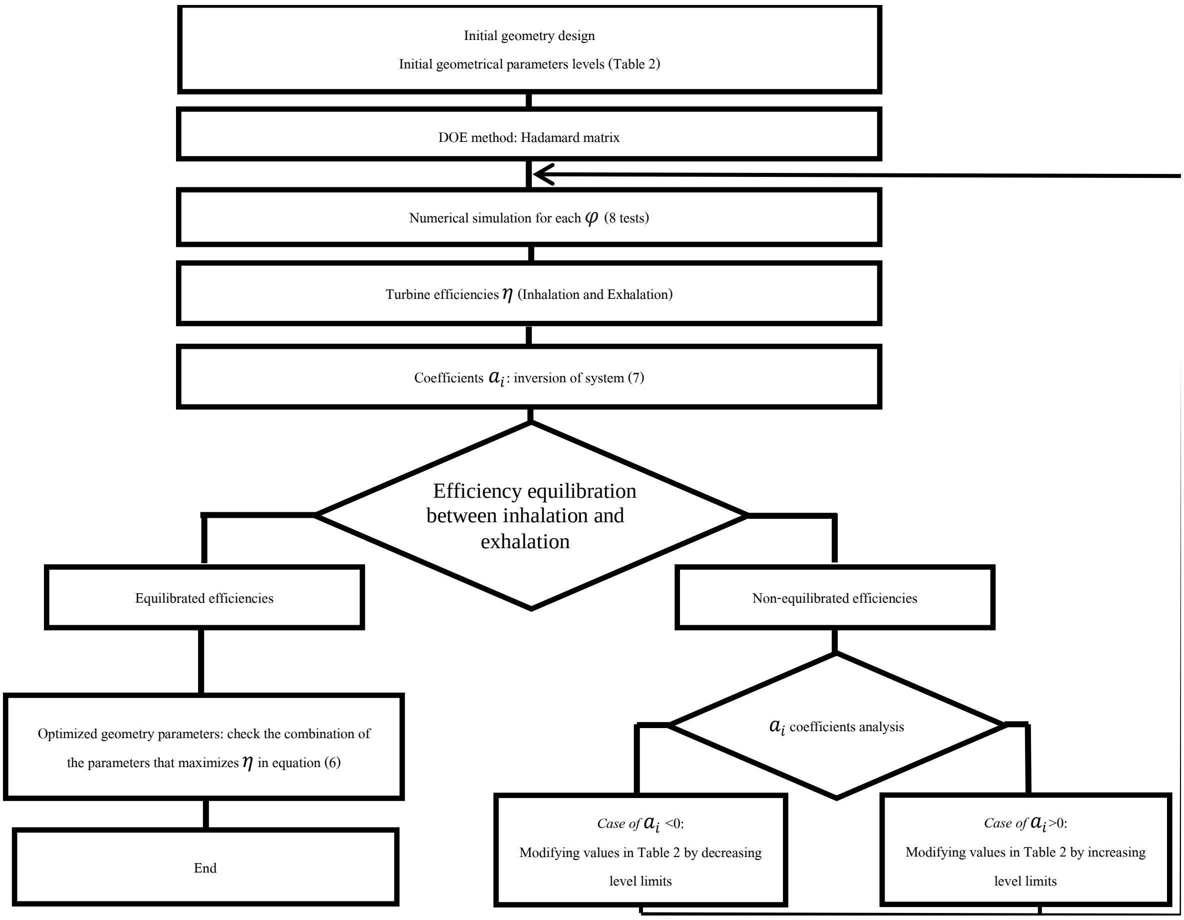

Fig. 5. The algorithm for the optimization process.

Table 5. Parameter level values for the second DOE (dimensionless values).

Level	R_p^r	l_r	β^*	d_c
-1	0.363	0.909	28°	0.582
1	0.436	1.1	32°	0.636

Table 6. Turbine efficiencies of the modified DOE for the eight tests in exhalation and inhalation modes.

	Tests:	1	2	3	4	5	6	7	8
	Efficiencies:	η_1	η_2	η_3	η_4	η_5	η_6	η_7	η_8
Inhalation, Flow rate: φ	-0.5	56.4	59	65.7	60.5	61.8	56.2	61.7	57.2
	-1	61	62.9	65	58.6	63.3	57.4	63	61
	-1.5	58.8	58.9	61	57	59.4	53.9	61.5	57.1
	-2	56	56	58.4	54	56.8	52.8	58.2	54.7
	-2.5	53.9	54	55.8	52	54.8	51.4	55.8	52.8
Exhalation, Flow rate: φ	0.5	49	56.3	55.8	49	60.2	46	50.8	60.9
	1	58	56.2	57.5	49.4	63	49.2	60.5	61.8
	1.5	57.6	52.9	56.4	49	59	49	59.4	58.4
	2	55.8	50.8	54.4	48	56.4	48	57.5	56.1
	2.5	54.1	49	52.8	47	54.5	47	56	54.1

From Table 4 and according to the algorithm of optimization (Figure 5), the level limits of the parameter R_p^r will be decreased because its corresponding coefficient a_2 takes negative values in both functioning modes.

For the parameters l_r and d_c, their level limits will be increased because their corresponding coefficients a_3 and a_5 take mostly positive values for the two modes. Although the coefficient a_4 corresponding to the parameter β^* takes equilibrate values between the two modes, its level limits will be narrowed in order to refine its optimal value. For this, a second experimental design has been elaborated with the new parameter levels.

2.2.6 The modified design and results

With the same method, the second DOE has been elaborated. The new parameter levels are presented in Table 5.

From the additional numerical tests results for the turbine efficiencies (Table 6), the coefficients a_i

(i=1,…,5) are calculated and presented in the Table 7 for exhalation and inhalation modes.

With the same analyse, a decrease of the level values of the parameters R_p^r and β^*, and an increase of those of l_r are recommended. For the parameter d_c, its level limits will be unmodified since the values of its corresponding coefficient are equilibrated between inhalation and exhalation. But according to drawings constraints limitations, the increase of the parameter R_p^r and the decrease of the parameter l_r are geometrically unrealisable. For that one parameter can be modified, which is β^*.

2.3 Optimization and Results

From the results of the second experimental design, a program has been elaborated with MATLAB in order to determine the optimal combination(s) of the four input parameters that maximize(s) the turbine efficiency for the two functioning modes (inhalation and exhalation).

The objective equation is (6) and variable inputs are those of the experimental design. These parameters have been varied within the two levels specified in Table 5 by increments of 1 mm for R_p^r, l_r and d_c, and 2° for β^*.

The optimal combinations for different flow coefficients in both functioning modes are presented in Table 8.

From Table 8, a couple of combinations that maximize the turbine efficiency can be identified as: C1= (0.363; 1.1; 28°; 0.582) and C2= (0.363; 1.1; 28°; 0.636).

The rotor blade design of the optimized configuration with different dimensionless values of the four parameters is presented in Figure 6.

Table 7. The coefficients a_i , i =1,…,5 for the modified DOE.

	φ	a_1	a_2	a_3	a_4	a_5
inhalation	-0.5	60	-1.1	0.1	-0.5	1.9
	-1	61	-1.5	1.0	0.05	0.8
	-1.5	58	-0.6	1.2	-0.3	1.1
	-2	56	-0.6	0.9	-0.06	0.79
	-2.5	54	-0.5	0.8	-0.04	0.59
Exhalation	0.5	53	-4.8	0.6	-1.72	-0.5
	1	57	-2.7	2.5	-1.72	-1.1
	1.5	55	-1.4	2.0	-1.24	-0.8
	2	53	-1.0	1.7	-1.1	-0.7
	2.5	52	-0.8	1.6	-1.09	-0.6

Table 8. Dimensionless values of optimal combinations for different flow coefficients for inhalation and exhalation.

	Exhalation (R_p^r; l_r;□β^*; d_c)	Inhalation (R_p^r; l_r;□β^*; d_c)
$\lvert\varphi\rvert$=0.5	(0.363;1.1;28°;0.582)	(0.363; 50; 28°; 0.636)
$\lvert\varphi\rvert$=1	(0.363; 1.1; 28°;0.582)	(0.363; 1.1; 32°; 0.636)
$\lvert\varphi\rvert$=1.5	(0.363; 1.1; 28°; 0.582)	(0.363; 1.1; 28°; 0.636)
$\lvert\varphi\rvert$=2	(0.363; 1.1; 28°; 0.582)	(0.363; 1.1; 28°; 0.636)
$\lvert\varphi\rvert$=2.5	(0.363; 1.1; 28°; 0.636)	(0.363; 1.1; 28°; 0.636)

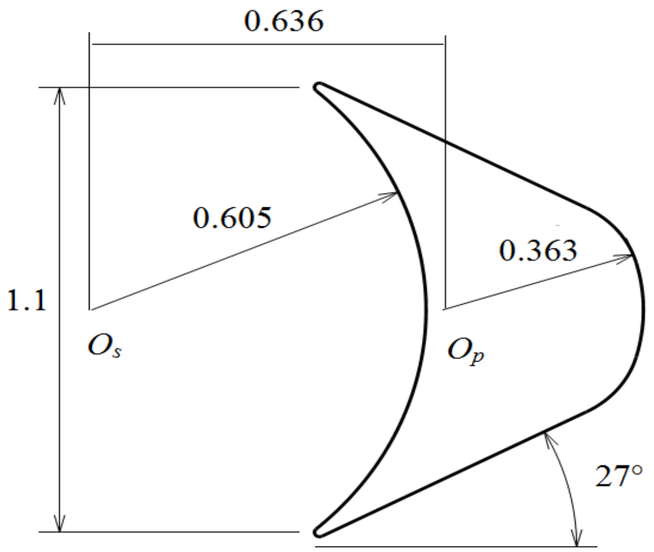

Fig. 3. The optimized rotor blade profile of the self-rectifying radial impulse turbine (dimensionless values).

In order to compare the efficiency of the two proposed turbine configurations over the two functioning modes (inhalation / exhalation), additional numerical tests has been performed. Figure 7 shows their efficiency variation for different flow coefficients

From Figure 7, it can be noticed that the combination $C2$ has the maximum efficiency in the two functioning modes.

Additional tests with variation of the parameter β^* have been also performed on the combination $C1$. Five values have been tested ranging from 23° to 27°. The results have shown that the combination with β^*= 27° leads to the optimal efficiency. So, the optimal combination of the rotor blade corresponds to $(R_p^r; l_r; \beta^*; d_c)$ = (0.363; 1.1; 27°; 0.636).

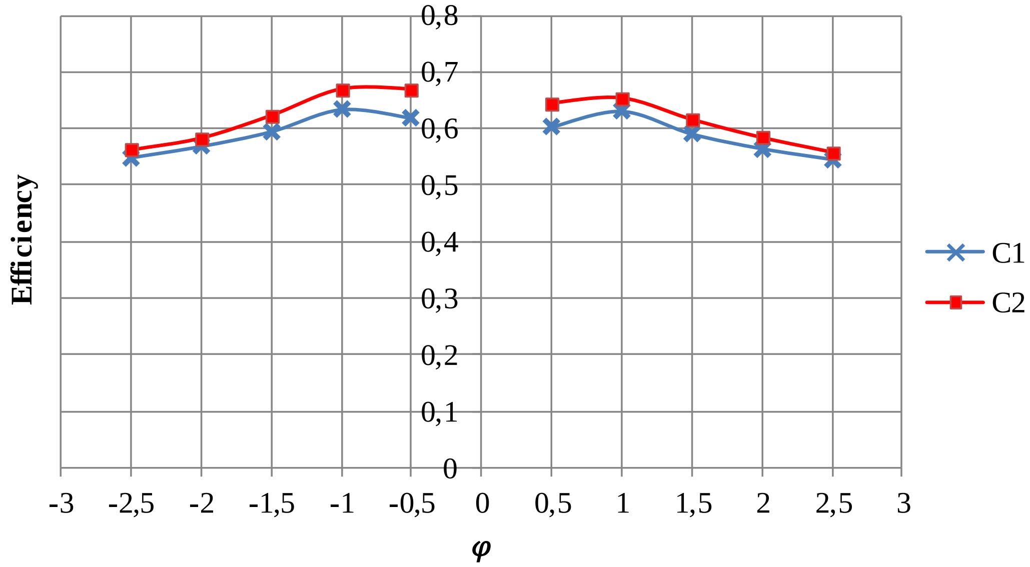

Fig. 4. The efficiency variation of the two proposed turbines for different flow coefficients.

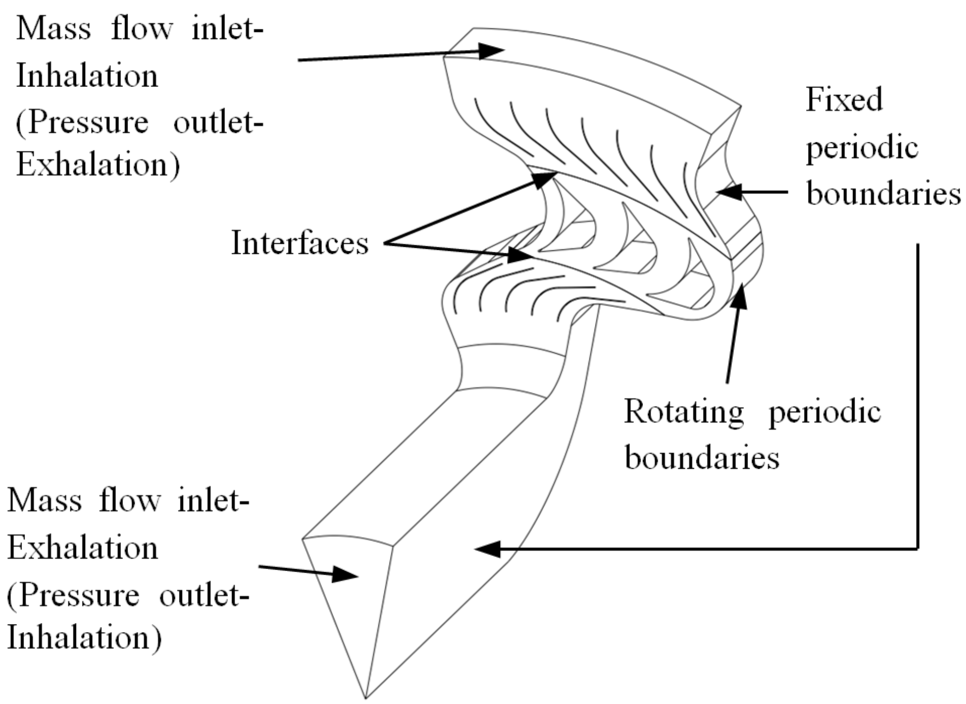

Fig. 5. 3D periodic domain and boundary conditions.

3. PERFORMANCE EVALUATION AND COMPARATIVE ANALYSIS

This subsection is focused on drawing up, firstly, the analysis of the flow characteristics and of the energetic performances of the present turbine with circular rotor blade profile and, secondly, to perform a comparison with those of a turbine designed with elliptical rotor blade profile whose characteristics are presented in [10].

Flow simulations are performed in 3D by means of ANSYS Fluent code. Flow is considered incompressible, viscous, 3D and steady. Since the turbine is axisymmetric and in order to reduce the variable storage memory, periodic domain has been adopted as computational domain (Figure 8). The periodic boundary conditions have been imposed in the circumferential direction as illustrated in Figure 8. Numerical tests can be performed without loss in accuracy by using periodic domain instead of the whole domain, as in reference [19]. An unstructured tetrahedral mesh of about 2 500 000 cells is used in the periodic domain. The boundary conditions adopted for these 3D simulations are the same as in 2D.

3.1 Performance Analysis

In order to evaluate the energy distribution over the turbine, percentages of the energy losses in the fixed components (DUCT, IGV and OGV) and the useful energy transferred by the rotor have been assessed. Figure 9 shows these results done in 3D simulations where the duct refers to the zone between the air chamber and the entrance to IGV (Figure 2), and the outlet refers to the zone between the OGV exit and the atmosphere. Observations of these graphs reveal principally that significant energy losses appear in the fixed components (Duct, IGV, OGV and the outlet), important energy losses occur in IGV and OGV for the exhalation and the inhalation modes respectively, but great amount of energy is lost in OGV for exhalation mode, energy available in the rotor is higher in the inhalation than in the exhalation modes and the level of useful energy is higher in the inhalation than in the exhalation. For a losses understanding purpose, a local flow analysis has been conducted over the turbine elements. The total pressure variation in the fixed elements: OGV, IGV and duct (Figure 10), and the relative total pressure variation in the moving element: the rotor (Figure 11) has been carried out. The analysis has concerned the mid-span of the blades for IGV, rotor and OGV, and the circumferential surface for the Duct. In order to reduce the field of analysis, two flow coefficients where the turbine efficiency is expected to be maximum for both modes; $\varphi = -1$ for inhalation and $\varphi = 1$ for exhalation have been chosen [18]. For the OGV, it can be noted that a large variation of the total pressure at the trailing edge in the exhalation mode that correspond to the boundary layer separation. In the inhalation mode, a small separation in the trailing edge is noticed due to the reduction of the space between successive vanes.

For the IGV, a considerable variation of the total pressure can be noticed at the element exit in exhalation mode, which causes significant losses at this zone. This variation is due to the geometrical form of the vane which is not adapted to the flow exit. For the inhalation mode, a reduced local flow separation has been observed at the trailing edge which is due to divergence of the area between successive guide vanes for the entrance to the exit of the element.

For the duct, a large flow separation can be noticed at the zone of the change of curvature of the flow from axial to radial. This is due to small radius of the superior connecting surface (Figure 10) between the axial and the radial channels.

An increase of the total pressure at the inferior connecting surface (Figure 10) corresponding to the flow resistance by the wall can be noted. This is due to the non-adapted value of the radius of this surface which is much reduced. For the inhalation mode, a reduced local flow separation can be noted at the superior connecting surface, which is due to the abrupt variation of the flow orientation from radial to axial. An important flow separation is remarked at the inferior connecting surface which is due to the large divergence of the area between the entrance and the exit of the duct.

For the rotor, a large variation of the relative total pressure at the trailing edge can be noted in the exhalation mode that leads to the boundary layer separation. This separation is due to the divergence of the inter-blade area from the leading to the trailing edges. At the leading edge, it can be also observed a local flow separation which is due to the non-adaptation of the relative flow angle. However, a reduced variation can be remarked at the trailing edge in the inhalation mode, which is due to the convergent inter-blade area from the leading to the trailing edges.

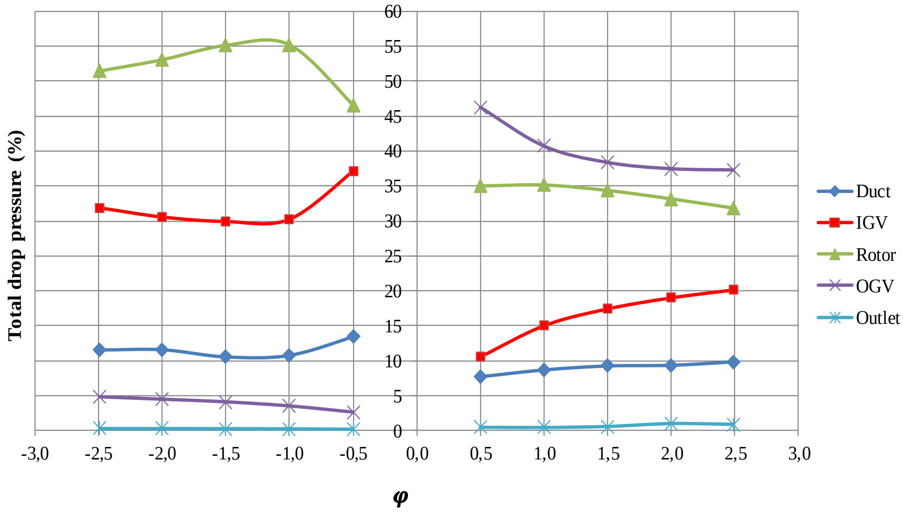

Fig. 6. Total drop pressure (%) in different components in the optimized turbine.

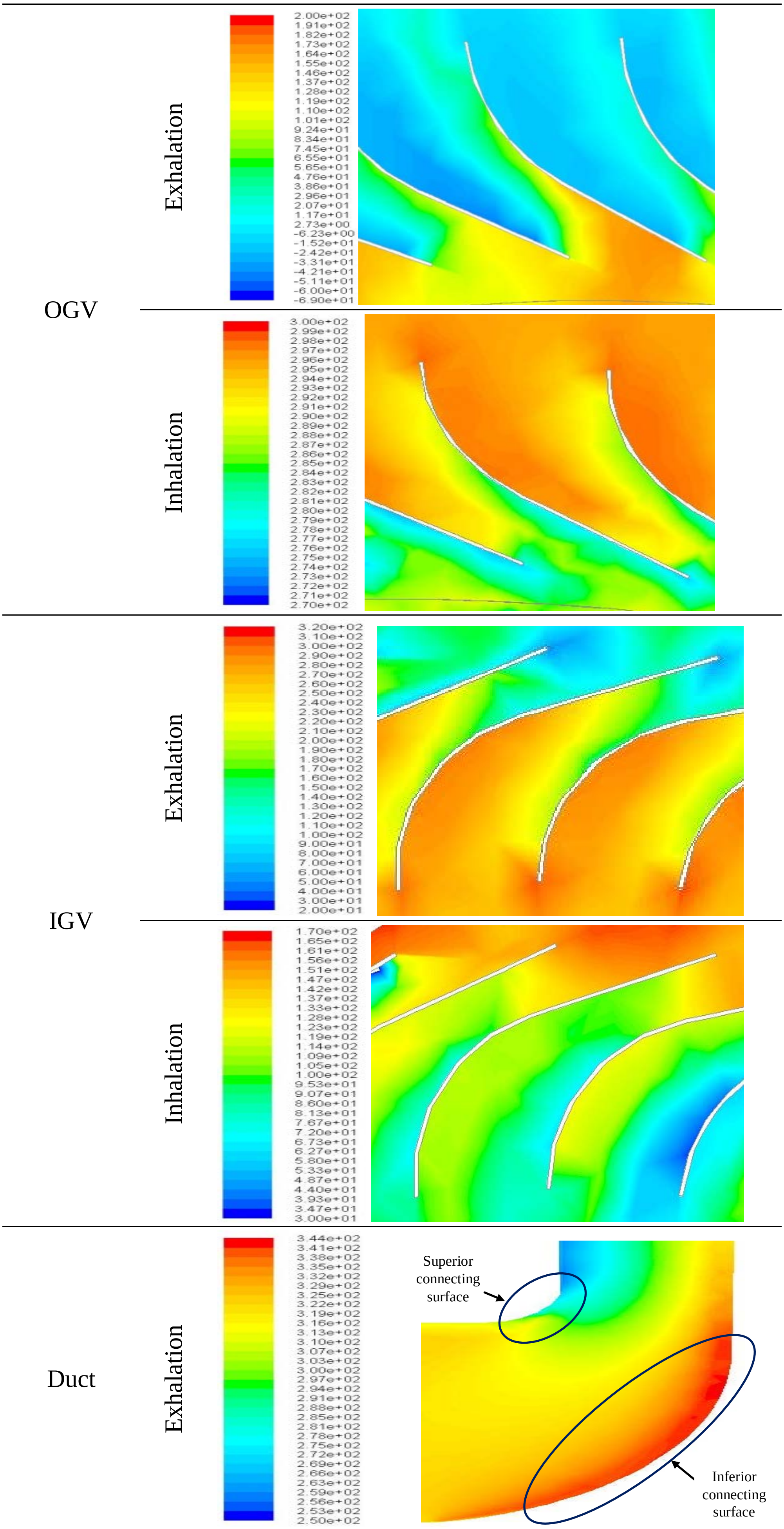
OGV
Exhalation
2.00e+02
1.91e+02
1.82e+02
1.73e+02
1.64e+02
1.55e+02
1.46e+02
1.37e+02
1.28e+02
1.19e+02
1.10e+02
1.01e+02
9.24e+01
8.34e+01
7.45e+01
6.55e+01
5.65e+01
4.76e+01
3.86e+01
2.96e+01
2.07e+01
1.17e+01
2.73e+00
-6.23e+00
-1.52e+01
-2.42e+01
-3.31e+01
-4.21e+01
-5.11e+01
-6.00e+01
-6.90e+01
Inhalation
3.00e+02
2.99e+02
2.98e+02
2.97e+02
2.96e+02
2.95e+02
2.94e+02
2.93e+02
2.92e+02
2.91e+02
2.90e+02
2.89e+02
2.88e+02
2.87e+02
2.86e+02
2.85e+02
2.84e+02
2.83e+02
2.82e+02
2.81e+02
2.80e+02
2.79e+02
2.78e+02
2.77e+02
2.76e+02
2.75e+02
2.74e+02
2.73e+02
2.72e+02
2.71e+02
2.70e+02
IGV
Exhalation
3.20e+02
3.10e+02
3.00e+02
2.90e+02
2.80e+02
2.70e+02
2.60e+02
2.50e+02
2.40e+02
2.30e+02
2.20e+02
2.10e+02
2.00e+02
1.90e+02
1.80e+02
1.70e+02
1.60e+02
1.50e+02
1.40e+02
1.30e+02
1.20e+02
1.10e+02
1.00e+02
9.00e+01
8.00e+01
7.00e+01
6.00e+01
5.00e+01
4.00e+01
3.00e+01
2.00e+01
Inhalation
1.70e+02
1.65e+02
1.61e+02
1.56e+02
1.51e+02
1.47e+02
1.42e+02
1.37e+02
1.33e+02
1.28e+02
1.23e+02
1.19e+02
1.14e+02
1.09e+02
1.05e+02
1.00e+02
9.53e+01
9.07e+01
8.60e+01
8.13e+01
7.67e+01
7.20e+01
6.73e+01
6.27e+01
5.80e+01
5.33e+01
4.87e+01
4.40e+01
3.93e+01
3.47e+01
3.00e+01
Duct
Exhalation
3.44e+02
3.41e+02
3.38e+02
3.35e+02
3.32e+02
3.29e+02
3.25e+02
3.22e+02
3.19e+02
3.16e+02
3.13e+02
3.10e+02
3.07e+02
3.03e+02
3.00e+02
2.97e+02
2.94e+02
2.91e+02
2.88e+02
2.85e+02
2.81e+02
2.78e+02
2.75e+02
2.72e+02
2.69e+02
2.66e+02
2.63e+02
2.59e+02
2.56e+02
2.53e+02
2.50e+02
Superior connecting surface
Inferior connecting surface

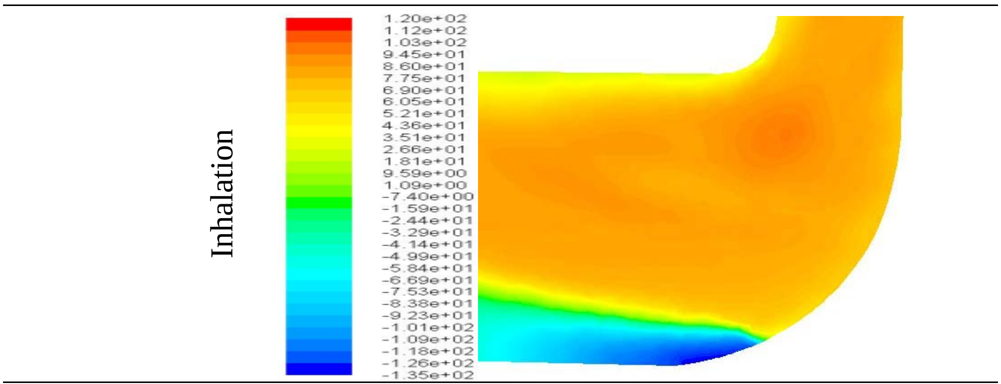

Fig. 7. Absolute total pressure (Pa) contour of the flow passing through OGV, IGV and the duct.

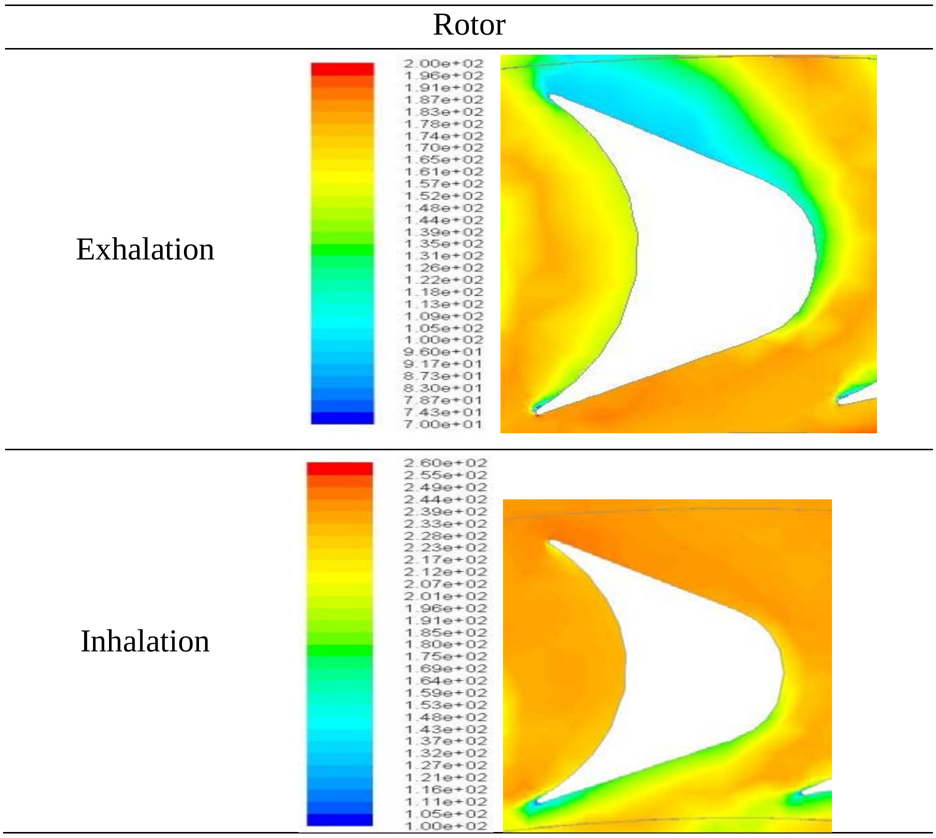

Fig. 8. Relative total pressure (Pa) contour of the flow passing through the rotor blades.

3.2 Turbines Performance Comparison

A performance comparison between the turbines with rotor designed with circular profiles developed in the present work and with elliptical profiles developed in [10]. Results correspond to the dimensionless coefficients for the total pressure (C_A) and the torque (C_T) (Figure 12), the turbine efficiency (Figure 13). Figure 12-a reveals that the coefficient C_A is reduced significantly in the turbine in both functioning modes; inhalation and exhalation, but more in inhalation, by using the optimized rotor with circular profiles instead of the previous one with elliptical profiles. This remark means that energy losses in terms of total pressure drop has been lessened at the improved rotor with circular profiles. From Figure 12-b, It can be noticed a slight reduction in the coefficient C_T in both modes for the improved rotor, which means a diminution of the useful energy in terms of the torque harnessed by the rotor. However, the turbine efficiency that is a ratio of the coefficients C_T and C_A (Equation 5) is increased in both functioning modes by using the optimized rotor with circular profiles instead of that with elliptical profiles; an increase of about 18% has been noticed on the peak efficiency for the inhalation mode, and a slight increase can be noted in the exhalation mode:

(a)

(b)

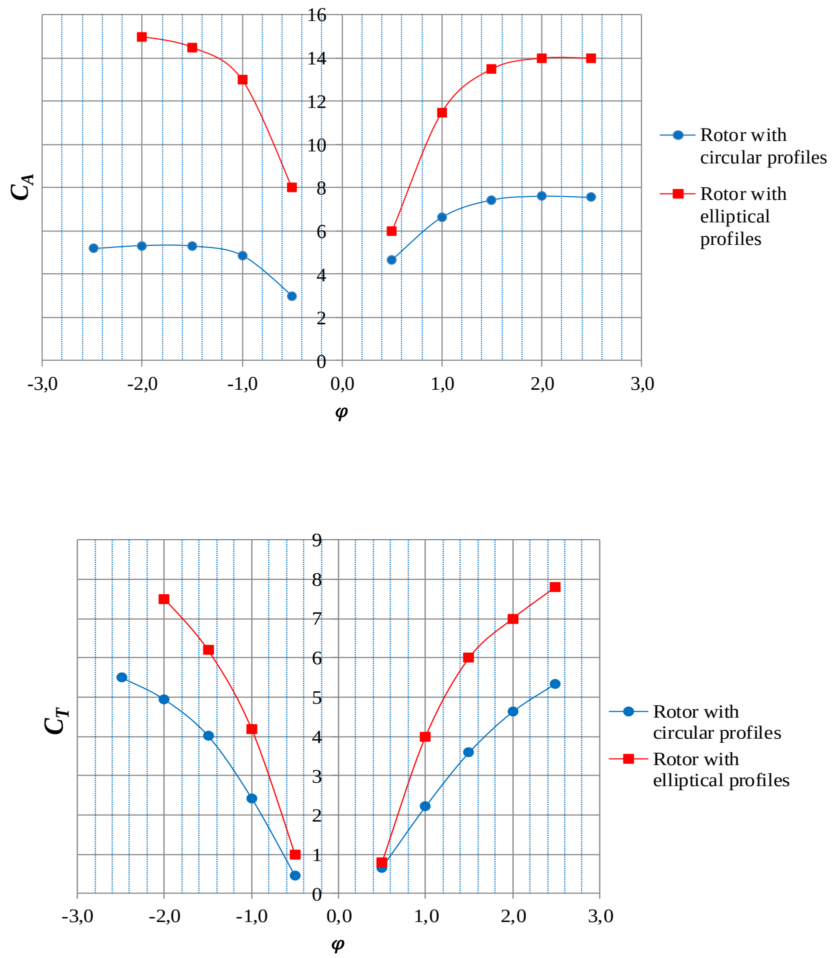

Fig. 9. (a) Turbine total pressure coefficient (C_A). (b) Turbine torque coefficient (C_T).

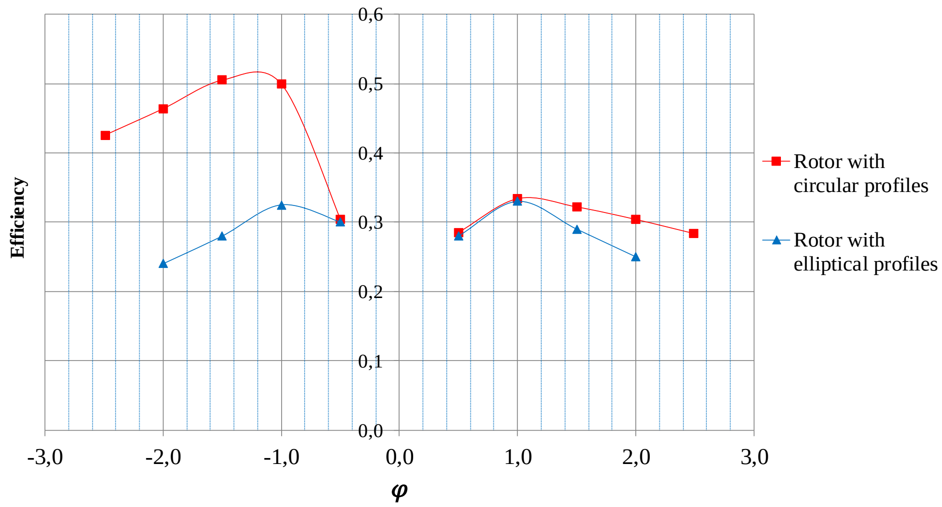

Fig. 10. Turbine efficiency.

4. CONCLUSIONS

In this paper, a brief presentation of the OWC turbines design evolution has been done over the last years. Many novel designs with higher performances have been introduced. For this work, a rotor blade optimization has been performed for the impulse radial turbine, which has low manufacturing cost and simple design. The experimental design method (DOE) has been used for the optimization process in order to maximize the turbine efficiency. The tests have been done in 2D numerical simulation with ANSYS Fluent. Four design parameters have been chosen as inputs in the optimization procedure; the radius of the suction side, the blade chord, the inter-centres of the two circular arcs, and the geometrical angle in the leading and trailing edges of the blade rotor, and one as output; the turbine efficiency. The other blade parameters (IGV and OGV) are kept unchanged. An optimizing algorithm with MATLAB code has been elaborated and an optimized combination of these four parameters has been obtained that maximizes and equilibrates the turbine efficiency in the two functioning modes; inhalation and exhalation.

According to the performance and flow analyses of the turbine with the improved rotor, it has been found that the fixed elements; the duct, IGV and OGV reveal important energy losses. These losses are caused principally by the not adapted geometrical forms of these elements for minimizing the flow losses at the entrance and exit for IGV and OGV, and at the connecting surfaces of the change of curvature from radial to axial direction, or vice-versa. The space between successive guide vanes is not kept uniform can be mentioned as another problem for these elements, which leads to the flow detachment at its trailing edges. For the moving element, a boundary layer separation has been noticed in the trailing edge for functioning modes, inhalation and exhalation. This flow separation is caused essentially by the increase of the space between successive blades.

A brief performance comparison has been dropt between the turbines with improved and previous rotors. Results reveal that the total drop pressure has been reduced significantly by using the optimized rotor with circular profiles instead of the elliptical one. This improvement has leaded to an increase of about 18% on the peak efficiency in the inhalation mode.

For the future research works, additional experimental designs for optimizing the duct and the guide vanes profiles will be elaborated. Keeping the space between successive blades for IGV, rotor and OGV could avoid the boundary layer separation in its trailing edges, and therefore equilibrating and improving the turbine efficiency in both functioning modes; exhalation and inhalation.

ACKNOWLEDGEMENT

This research work has been conducted as part of the research activity within the EMISys research team at the Turbomachinery Lab with the institutions financial support of Mohammadia School of Engineers and Mohammed V University in Rabat.

REFERENCES

[1] Hans-Wilhelm S., 2016. World Energy Resources Marine Energy, *World Energy Council*, United Kingdom.

[2] Bouhrim H. and A. El Marjani. 2015. Turbine-Chamber Interactions Analysis in an OWC device for Wave Energy Conversion, *3rd International Renewable and Sustainable Energy Conference*, Marrakech and Ouarzazate, December 10-13, IEEE.

[3] De Falcão A.F.O., 2010. Wave energy utilization: A review of the technologies. *Renewable and Sustainable Energy Reviews* 14: 899-918.

[4] Wells A.A., 1976. Fluid driven rotary transducer. *British Patent 1595700*.

[5] Raghunathan S., 1975. The wells turbine for wave energy conversion. *Progress in Aerospace Sciences* 31: 31–335.

[6] Babinstev I.A., 1975. Apparatus for converting sea wave energy into electrical energy. *U.S. Patent 3922739*.

[7] McCormick M.E., Rehak J.G., and Williams B.D., 1992. An experimental study of a bi-directional radial turbine for pneumatic conversion, *Mastering Ocean through Technology* 2: 866–870.

[8] McCormick M.E. and B. Cochran. 1993. A performance study of a bi-directional radial turbine. In the *Proceedings of the European Wave Energy Symposium, East Kilbride, Scotland*. 21-24 May, 443–448.

[9] Dixon S.L. and C.A. Hall. 2010. *Fluid mechanics and thermodynamics of turbomachinery*, Elsevier.

[10] Pereiras B., Castro F., El Marjani A., and Rodríguez M.A., 2011. An improved radial impulse turbine for OWC. *Renewable Energy* 36(5): 1477–1484.

[11] Takao M., Takami A., Okuhara S., and Setoguchi T., 2011. A twin unidirectional impulse turbine for wave energy conversion. *Journal of Thermal Science* 20: 394-397.

[12] Natanzi S., Teixeira J., and Laird G., 2011. A Novel high-efficiency impulse turbine for use in oscillating water column devices. In the *Proceedings of the 9th European Wave Tidal Energy Conference* Southampton, United Kingdom, 5-9 September.

[13] Falcão F.O., Gato L.M.C., and Nunes E.P.A.S., 2013. A novel radial self-rectifying air turbine for use in wave energy converters. *Renewable Energy* 50: 289–298.

[14] Falcão F.O., Gato L.M.C., and Nunes E.P.A.S., 2013. A novel radial self-rectifying air turbine for use in wave energy converters. Part 2. Results from model testing. *Renewable Energy* 53: 159–164.

[15] Falcão F.O., Gato L.M.T., Henriques J.C.C., Borges J.E., Pereiras B., and Castro F., 2015. A novel twin-rotor radial-in flow air turbine for oscillating-water- column wave energy converters. *Energy* 93: 2116–2125.

[16] Das T.K., Halder P., and Samad A., 2017. Optimal design of air turbines for oscillating water column wave energy systems : A review. *Journal of Ocean and Climate: Science, Technology and Impacts* 8: 37–49.

[17] Goupy J. 1993. *Methods for Experimental Design. Principles and Applications for Physicists and Chemists*, Elsevier.

[18] Setoguchi T., Santhakumar S., Takao M., Kim T.H., and Kaneko K., 2002. A performance study of a radial turbine for wave. *Proceedings of the*

Institution of Mechanical Engineers, Part A: Journal of Power and Energy 216: 15–22.

[19] El Marjani A., Castro Ruiz F., Rodriguez M.A., and Parra Santos M.T., *2008*. Numerical modelling in wave energy conversion systems. *Energy* 33: 1246–1253.

[20] Setoguchi T., 2001. A review of impulse turbines for wave energy conversion. *Renewable Energy* 23: 261–292.

[21] Uzol O. and C. Camci. 2005. Heat transfer, pressure loss and flow field measurements downstream of staggered two-row circular and elliptical pin fin arrays. *Journal of Heat Transfer* 127: 458–471.

[22] Lundstedt T., 1998. Experimental design and optimization, *Chemometrics and Intelligent Laboratory Systems* 42: 3–40.